

Experimental Investigation of a Low Frequency Instability in a Modified Penning Discharge (Q-PIG) *

F. KLAN

Institut für Plasmaphysik, Garching bei München

(Z. Naturforsch. 25 a, 263—273 [1970]; eingegangen am 28. November 1969)

Low frequency oscillations observed in a modified PIG discharge were identified as fluctuations of the electron temperature. These oscillations only occurred under certain conditions (low gas pressure, relatively high magnetic field), whereas at high pressure and low magnetic field strength the plasma was remarkably stable; this is why the discharge is referred to as a "quiescent" PIG (Q-PIG) discharge. This paper describes measurements for obtaining a detailed picture of the two modes of the discharge. A qualitative explanation of the phenomena observed is obtained using the energy balance of the electron gas.

1. Introduction

The Penning (or PIG) discharge is subject to various kinds of instabilities. Both high frequency instabilities of the two-stream type¹ and low frequency drift instabilities^{2, 3} have been found and investigated. This paper describes the experimental investigation of a Penning discharge with modified electrode geometry. This discharge differs as follows from other Penning discharges treated in the literature:

1. There exists a stable state with extremely low electron temperature.
2. The radial electric field is very small in spite of the high operating voltage.
3. There is an instability of very low frequency which disturbs the electron temperature, while the electron density remains constant in time⁴.

By contrast, in most PIG discharges both the electron temperature and the radial electric field strength, and hence the azimuthal $\mathbf{E} \times \mathbf{B}$ drift of the charged particles, are more than ten times as high. The instabilities were identified as perturbations of the plasma density, the electron temperature being assumed to be constant.

This paper describes in Sect. 2 the basic mechanism of a Penning discharge. In the next three Sec-

tions (3 to 5) the modified electrode geometry and the special properties of the so-called Q-PIG are discussed and some technical details are given. Sect. 6 is concerned with the measurements which have been performed in order to determine the temperature and density distributions in the periodically oscillating state. The conditions for the transition from this unstable state to the stable one are discussed in Sect. 7, whereas in Sect. 8 the axial extension of the temperature distribution is investigated. The next two sections describe two additional experiments; one of them is concerned with the external excitation of a temperature oscillation (9), the other deals with a particular method to measure the radial electric field (10). A qualitative explanation of the experimental results is presented in Sect. 11 and in Sect. 12 the Q-PIG discharge is compared with other discharges.

2. Mechanism of a Penning discharge

An electrode geometry frequently used for Penning discharges is shown in Fig. 1. A similar model serves as the basis of, for example, the calculations of HOH⁸. In stationary operation with cold cathodes the ions impinging on the cathodes result in the emission of secondary electrons which are accele-

Sonderdruckanforderungen an Dr. F. KLAN, Institut für Plasmaphysik, D-8046 Garching bei München.

* Auszug aus einer von der Fakultät für Maschinenwesen und Elektrotechnik der Technischen Hochschule München genehmigten Dissertation.

¹ G. BRIFFOD, M. GREGOIRE, and S. GRUBER, Plasma Physics (J. Nucl. Energy, Pt. C) 6, 329 [1964].

² F. F. CHEN and A. W. COOPER, Phys. Rev. Lett. 9, 333 [1962].

³ K. I. THOMASSEN, Phys. Rev. Lett. 14, 587 [1965].

⁴ This instability was first reported at the 8th Conf. on Phenomena in Ionized Gases in Vienna⁵; other experiments⁶ and theoretical investigations⁷ were reported at the 9th Conf. P.I.G. in Bucharest 1969.

⁵ F. KLAN, VIII. Conf. P.I.G., Vienna 1967, p. 190.

⁶ F. KLAN, IX. Conf. P.I.G., Bucharest 1969, p. 247.

⁷ F. KLAN, IX. Conf. P.I.G., Bucharest 1969, p. 246.

⁸ F. C. HOH, Phys. Fluids 6, 1184 [1963].



Dieses Werk wurde im Jahr 2013 vom Verlag Zeitschrift für Naturforschung in Zusammenarbeit mit der Max-Planck-Gesellschaft zur Förderung der Wissenschaften e.V. digitalisiert und unter folgender Lizenz veröffentlicht: Creative Commons Namensnennung-Keine Bearbeitung 3.0 Deutschland Lizenz.

Zum 01.01.2015 ist eine Anpassung der Lizenzbedingungen (Entfall der Creative Commons Lizenzbedingung „Keine Bearbeitung“) beabsichtigt, um eine Nachnutzung auch im Rahmen zukünftiger wissenschaftlicher Nutzungsformen zu ermöglichen.

This work has been digitalized and published in 2013 by Verlag Zeitschrift für Naturforschung in cooperation with the Max Planck Society for the Advancement of Science under a Creative Commons Attribution-NoDerivs 3.0 Germany License.

On 01.01.2015 it is planned to change the License Conditions (the removal of the Creative Commons License condition "no derivative works"). This is to allow reuse in the area of future scientific usage.

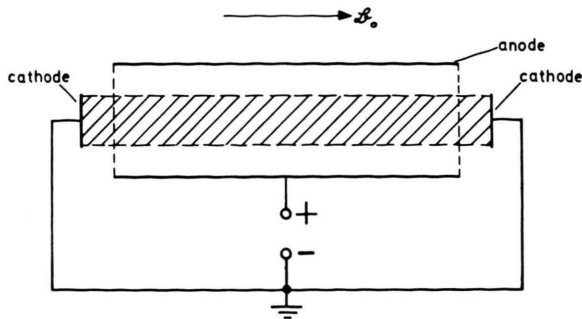


Fig. 1. Electrode geometry of a conventional PIG discharge.

rated in the cathode fall region to energies of more than 100 eV. At sufficiently low neutral gas pressure — Penning discharges are frequently operated at pressures of 10 to 100 mTorr — the mean free paths are so long that fast electrons can advance to the opposite cathode almost without loss of energy. Because of the symmetry of the electrode geometry the electrons oscillate back and forth between the two cathodes and are prevented by the magnetic field from escaping radially. By ionizing the neutral atoms the electrons trapped in this way produce a plasma which occupies the hatched region in Fig. 1. The ions of this plasma move parallel to the magnetic field and reach the cathodes, where they are neutralized. The electrons, on the other hand, have to diffuse perpendicularly to the magnetic field in order to reach the anode, i. e. their transverse mobility is severely impaired. In a PIG discharge with the electrode geometry of Fig. 1 a radial electric field of several V/cm builds up which forces the electrons to move towards the anode. At the same time this field together with the axial magnetic field causes an $\mathbf{E} \times \mathbf{B}$ drift of the charged particles in the azimuthal direction which sets the whole plasma in rotation relative to the neutral gas at rest. As a result of the different interaction of the electrons and ions with the neutral gas, any density fluctuation will produce local charge separation. The resulting space charge field is directed in such a way that the plasma is driven radially outwards. HOH⁸ and SIMON⁹ have shown that this situation will lead to instability if the radial electric field and hence the rotational velocity of the charged particles is sufficiently high. In general, the low frequency instabilities observed in many Penning discharge can readily be explained in terms of this mechanism.

⁹ A. SIMON, Phys. Fluids 6, 382 [1963].

3. Modified Penning discharge

In order to avoid the instability just described, the electrode geometry of Fig. 2 was chosen. In such a geometry the electric field is essentially concentrated in the cathode region, whereas the actual plasma is almost free of electric fields. This was confirmed by measurements. However, the discharge mechanism is still the same as in conventional Penning discharges because a direct discharge between a cathode

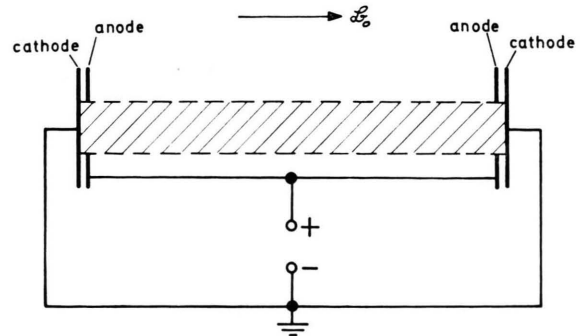


Fig. 2. Electrode geometry of the modified PIG discharge (Q-PIG).

and its anode is not possible owing to the smallness of the gap (≈ 1 mm) and the low gas pressure ($p \approx 30$ mTorr). This geometry was used for a stationary helium discharge the parameters of which varied within the following ranges:

$$p = 20 \dots 100 \text{ mTorr}, \quad B = 200 \dots 600 \text{ gauss}, \\ U_b = 500 \dots 1000 \text{ V}, \quad n_e = 10^{12} \dots 10^{13} \text{ cm}^{-3}, \\ i_d = 100 \dots 1000 \text{ mA}, \quad T_e = 1500 \dots 12\,000 \text{ }^\circ\text{K};$$

here U_b is the operating voltage and i_d the discharge current, the other symbols having their usual meaning.

4. The Special Properties of the Modified Penning discharge

At high pressure ($p \approx 60$ mTorr) and low magnetic field ($B \approx 300$ gauss) the plasma looks very quiescent and stable. This impression is also confirmed by the oscillograms of the discharge current, operating voltage, and floating potential of electrostatic probes. The electron density was measured with microwaves and Langmuir probes, and the electron temperature was determined from the current-voltage characteristic of a Langmuir probe. Both parameters were measured as a function of the radius; for the density this yielded a function decreas-

ing monotonically outwards, similar to a zeroth order Bessel function, while the temperature was practically independent of the radius, but extremely low (approx. 2000 °K). Because of its similarity to alkali plasmas (stability, low temperature) the modified Penning discharge is referred to as Q-PIG (Q = quiescent, PIG = Philips ionization gauge). If the pressure is lowered, the properties of the discharge change appreciably. The floating potential of the probe is now no longer constant in time, but exhibits periodic fluctuations with a frequency of about 1 kHz; similar fluctuations are also observed in the discharge current and in most of the other parameters. The change from the stable state (A) to the periodically oscillating state (B) occurs suddenly at a certain pressure; it can also be induced by *increasing* the magnetic field at constant pressure. If the magnetic field is increased or the pressure reduced even more, the discharge assumes a highly turbulent state (C). An irregularly flickering luminosity and incoherent high and low frequency fluctuations of the probe potential are observed. Since no reliable experimental results could be expected in this "chaotically unstable" state, only the states A and B were investigated. One of the main purposes of this investigation was to find the cause of the unusually coherent and reproducible signals in state B.

5. Some Technical Details of the Q-PIG discharge

The arrangement of the cathode system is shown in Fig. 3. The actual cathode is a molybdenum disc welded into a stainless steel support ring. The support is mounted on an aluminium block which can be cooled with water. An aluminium case for holding the anode

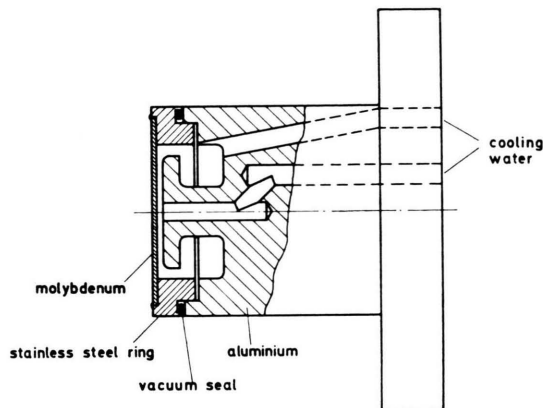


Fig. 3. Arrangement of the watercooled cathode systems.

is slipped over the whole cathode block (see Fig. 4). The anode itself is an aluminium ring 10 mm thick with an inner (anode) diameter of 50 mm. Anode ring and cathode disc are separated by a gap of 1 mm only.

Two such systems are incorporated in a vacuum vessel consisting of three parts (Fig. 4). In the centre there is an aluminium ring with four side ports through which probes, microwave antennae and the like can be admitted; one of these apertures was usually used for connecting the pumping system. Two glass tubes with an inner diameter of 102 mm form vacuum tight connections on each side of the central ring. The ends of these tubes also form vacuum tight connections with the electrode systems. The total length of the vessel is approximately 80 cm, the distance between the cathodes approximately 50 cm.

6. Experimental Investigation of the Q-PIG Plasma

The most important plasma parameters, density and electron temperature, were measured in the stable state (A) first. The details will be dispensed

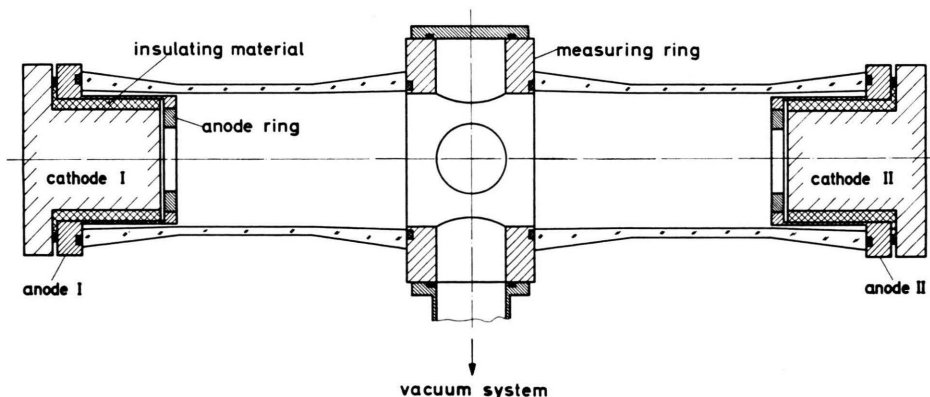


Fig. 4. Arrangement of the discharge tube.

with here in favour of the more interesting measurements in state B. (For a detailed account of all measurements see ¹⁰. In this state Langmuir probes showed periodic fluctuations of the ion saturation current but in the beginning it was not known, whether the plasma density or the electron temperature or perhaps both quantities were fluctuating. For largely negative probe potentials we have:

$$i_+ \propto n \sqrt{T_e} \quad (1)$$

where i_+ is the ion saturation current, n is the ion density and T_e is the electron temperature. In most instabilities the density is disturbed, while the electron temperature remains constant in time. In this case the fluctuations in the ion saturation current are a measure of the fluctuations in density. In order to check whether the assumption of constant electron temperature is in fact satisfied, the temperature was measured first at a fixed point as a function of time. The method used is illustrated in Fig. 5. The probe is kept at a negative potential of

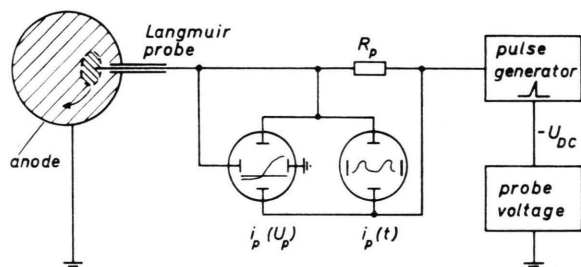


Fig. 5. Block diagram of the electronic system used for the time resolved measurement of the electron temperature.

about -10 V by a d. c. voltage source. A current i_p flows through the resistance R_p and causes a voltage drop which is recorded on the upper trace of a dual-beam oscilloscope (Teletronix 555) as a function of time. In state B we therefore obtain a signal that is proportional to the periodic fluctuations of the probe current. Furthermore, in the lead to the probe there is a pulse generator for producing triangular voltage pulses with variable amplitude between 0 V and 60 V. The rise and fall times of the pulse can be set independently between $3 \mu\text{sec}$ and 10 msec , while the pulse repetition rate can be chosen arbitrarily by means of an external trigger signal. In the time resolved temperature measurements in state B the trigger signal was derived from the periodic fluctuations of the probe signal which were fed to the

upper trace of the oscilloscope. In addition, the special time base of the oscilloscope used allowed an arbitrary time delay of the voltage pulse at the probe with respect to the original signal of the probe current. The second trace of the oscilloscope was now used to record the current voltage characteristic of the probe. Here the horizontal deflection of the trace was controlled by the probe voltage, the vertical deflection by the probe current. It was thus possible to record the probe current on one and the same screen both as a function of time and, at a fixed time, as a function of the probe voltage; a typical oscillogram is shown in Fig. 6. Here the time taken to traverse the part of the characteristic essential for determin-

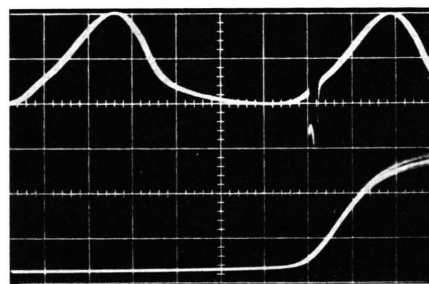


Fig. 6. Typical oscillogram of the probe current as function of time (upper trace, horiz. 0.2 ms/cm) and as function of probe voltage (lower trace, horiz. 1.43 V/cm).

ing the temperature, viz. the exponential part of the characteristic, was scarcely more than $10 \mu\text{sec}$, as careful investigations have shown. This time is, however, so short relative to the characteristic time of the fluctuations of the probe current (approx. $200 \mu\text{sec}$) that the method described may be regarded as "quasi-stationary". The characteristics, photographed with a Polaroid camera, were evaluated like stationary probe characteristics, and so practically instantaneous values of the electron temperature are obtained at any desired instant of time depending on the time delay of the trigger signal. A typical example for the evaluation of such a probe characteristic in the periodically oscillating state (B) is shown in Fig. 7.

The result of these temperature measurements over a period of the probe current signals was extremely surprising. It was found that there were highly pronounced fluctuations of the electron temperature with the same frequency and phase as those of the probe current and floating potential. The relationship between electron temperature and floating potential is shown in Fig. 8, where the circles are

¹⁰ F. KLAN, Lab.-Ber. IPP 3/92 [1969].

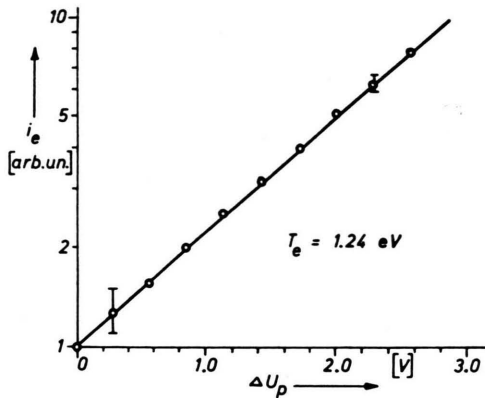
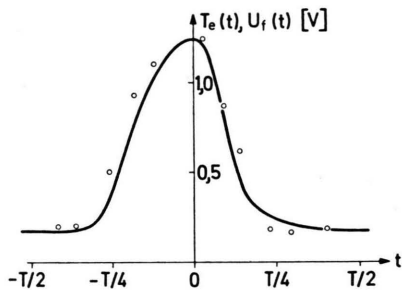


Fig. 7. Half-logarithmic plot of a typical probe characteristic.


 Fig. 8. Normalized floating potential and electron temperature as function of time (T being the reciprocal of the frequency of the periodic fluctuations).

the temperatures measured at the various times, while the solid curve represents the floating potential normalized so that $U_{f\max} - U_{f\min}$ just equals $(k/e) \cdot (T_{\max} - T_{\min})$. It is immediately obvious that the experimental points practically coincide with the normalized floating potential, i. e. the floating potential is a measure of the electron temperature. This well-known fact (cf., for example¹¹) was now used to measure the time fluctuations of the electron temperature at various points in the plasma in a much more simple way. The direct method described above was used to "calibrate" the floating potential in units of temperature: At each radius the temperature in the maximum and minimum was determined from the probe characteristic; the intermediate values were then simply taken from the normalized floating potential curve.

Comparison of the probe signals at various radii shows that the frequency is almost independent of the position of the probe. This means that the time dependent electron temperature measured at each

point can be transferred into one and the same coordinate system rotating with that frequency. This then gives an electron temperature distribution as a function of the radius and a polar angle φ , which is plotted in Fig. 9. Here the closed curves represent

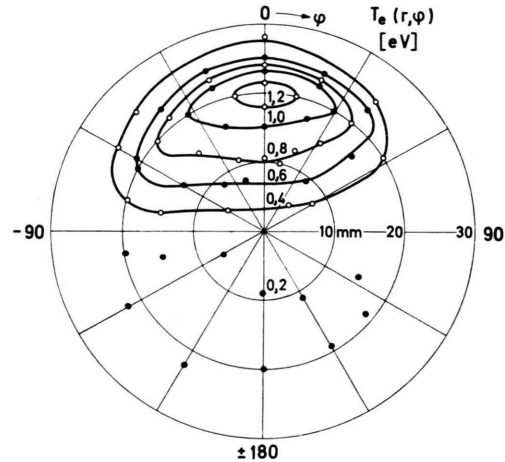


Fig. 9. Polar diagram of the transverse distribution of the electron temperature.

the isotherms of the electron gas measured in eV. The whole distribution rotates clockwise if the magnetic field is pointing into the drawing plane. If the magnetic field is reversed, the direction of rotation

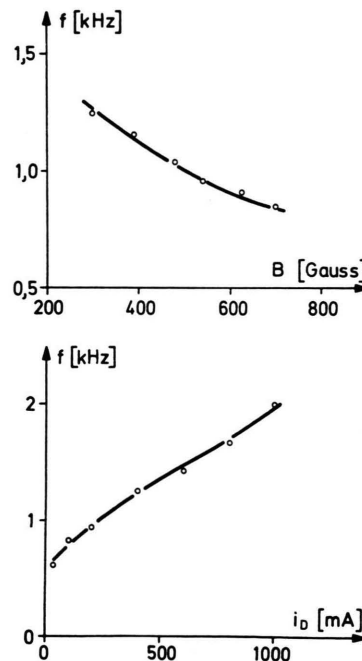


Fig. 10. Frequency of instability as function of magnetic field and discharge current.

¹¹ J. C. HOSEA, J. Appl. Phys. **37**, 2695 [1966].

is also reversed. The rotational frequency depends only slightly on the gas pressure; it decreases with increasing magnetic field, but increases with rising discharge current (Fig. 10).

A very similar picture is obtained if the ion saturation current is transferred to a polar diagram (Fig. 11). The closed lines here represent curves of equal current. In addition to the electron temperature distribution we may now determine the electron density distribution by substituting the values of i_+ and T_e from the diagrams in Figs. 9 and 11 point by point in Eq. (1). This equation yields only a relative distribution of the density; the absolute values were determined by comparison with microwave measurements (see ¹⁰). Surprisingly, this evaluation

yielded an almost rotational symmetric electron density distribution as shown in Fig. 12. The condition under which all of these measurements were made were as follows: helium gas pressure 26 mTorr, discharge current 100 mA, mean electron density $1.3 \times 10^{12} \text{ cm}^{-3}$, magnetic field 400 gauss.

7. Experimental Determination of the Instability Boundary

Whether the stable state (A) of the plasma or the unstable state (B) appears depends strongly on the pressure and magnetic field. As the change from state A to state B occurs very suddenly, it was not difficult to determine experimentally the boundary between the two by varying the pressure and magnetic field. The change from A to B occurs at somewhat lower pressure than the reverse process under otherwise equal conditions. Although this hysteresis does not matter very much, the critical values of pressure and magnetic field always refer to the change from the stable to the unstable state ($A \rightarrow B$). The discharge current was kept constant, while (1) the pressure was varied at constant magnetic field and (2) the magnetic field was varied at constant pressure. The transition points thus obtained are plotted in Fig. 13 in a λ, B plane; here λ is the mean free path of the electrons for elastic collisions with neutral helium atoms, which is inversely proportional to the gas pressure p :

$$\lambda [\text{cm}] = 57/p [\text{mTorr}] .$$

The measurements showed a distinct relationship between λ (or p) and B : The larger λ , i. e. the smaller the pressure, the weaker is the magnetic field at which transition takes place and vice versa. Above a pressure of about 70 mTorr, i. e. below a mean free

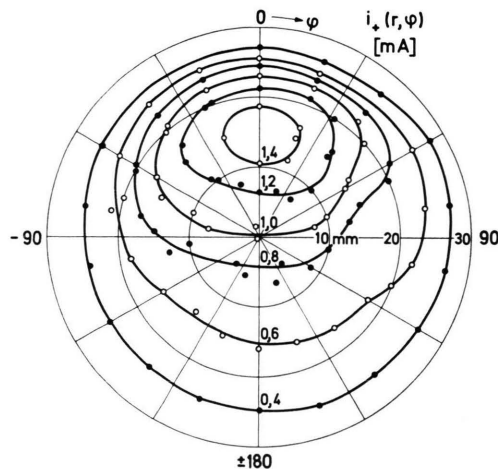


Fig. 11. Polar diagram of the transverse distribution of the ion saturation current.

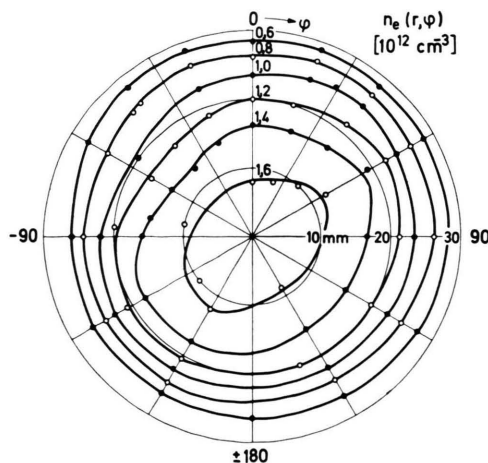


Fig. 12. Polar diagram of the transverse distribution of the plasma density.

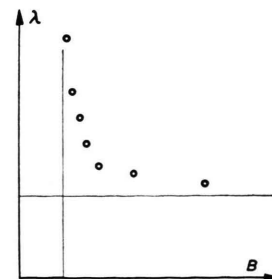


Fig. 13. Transition points between state A and B, plotted in a λ, B plane (λ being the mean free path for elastic collisions between electrons and neutrals, B being the magnetic field strength).

path of 0.8 cm, the plasma remains stable; the same is true below a magnetic field of 200 gauss. This is indicated in the figure by a horizontal and a vertical "asymptotic" line. The relation between λ and B is discussed qualitatively in a later section; a quantitative comparison with the theory is made in a further paper.

8. Investigation of the Axial Structure of the Electron Temperature Distribution

The measurements that yielded the transverse distributions in Fig. 9, 11, and 12 were made in the midplane of the discharge. The extent of these phenomena in the axial direction was investigated with two axially displaced probes (Fig. 14). The probes

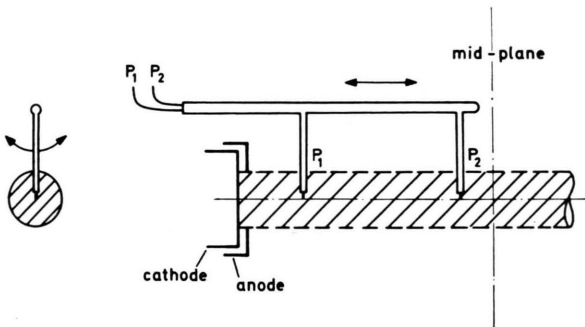


Fig. 14. Arrangement of the axially separated, movable probes.

P_1 and P_2 , mounted on a shaft 20 cm apart, could both be shifted axially and swept through the plasma, thereby covering a large part of the plasma volume. A comparison was made of the oscillograms of the floating potential of the two probes at various radii and in various z positions. The oscillograms were almost identical in all cases, as the typical example in Fig. 15 shows. From this it is concluded that the distributions measured in the centre extend almost unchanged to the cathodes and that there is no spiralling.

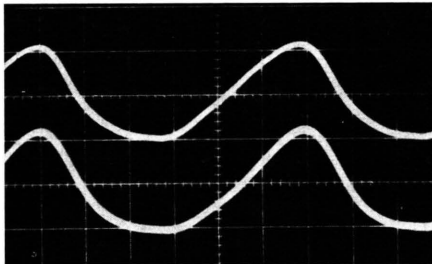


Fig. 15. Comparison of the time varying floating potentials of the two axially separated probes (horiz. 0.2 ms/cm).

9. Behaviour of a Temperature Perturbation in the Stable Plasma

The experiments described so far have shown that an anomalous, rotating temperature distribution sets in if the pressure or magnetic field exceeds a certain limit. It therefore seemed interesting to introduce from outside a small temperature disturbance of similar structure before this limit is reached, i. e. still in the stable state, and investigate its behaviour. For this purpose the following experiment was carried out: A small coaxial probe was placed at a point in the plasma at which the amplitude of the temperature fluctuations usually has a maximum (i. e. at $r \approx 20$ mm). The probe was connected by a coaxial cable to a microwave generator (frequency 1.7 to 4.1 GHz) which could be controlled with pulses of arbitrary length and frequency. The electrons could thus be brought locally for short times to temperatures up to 30% above the equilibrium temperature. Both the spatial concentration and the magnitude of the temperature rise were measured with a second probe; the region of elevated temperature extended perpendicularly to the magnetic field for about 1 cm, while the magnitude of the temperature rise was limited to values below 10% by reducing the microwave power.

Figure 16 shows a block circuit diagram of the set-up used. The Langmuir probes LP_1 and LP_2 were for detecting the fluctuations of the floating potential by means of the travelling temperature perturbation produced by the heating probe. The result of this experi-

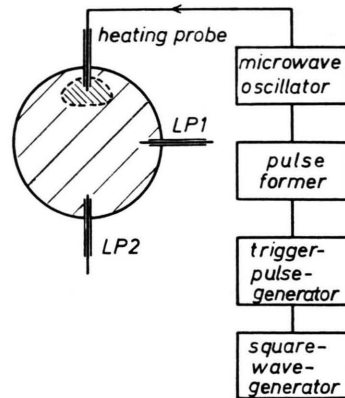


Fig. 16. Block diagram of the electronic system used for the local heating of the electrons.

ment is presented in Fig. 17. The upper trace in each oscillogram shows the fluctuations of the floating potential of one of the probes LP that are caused by a short microwave pulse (lower trace). The frequency of the damped oscillation ($f \approx 1$ kHz) is practically equal to that of the temperature fluctuations in state B; the direction of rotation of the temperature perturbation is also in agreement, as comparison between the signals from LP_1 and LP_2 showed. The lower the gas pressure (i. e. the longer the mean free path) the less damped

are the signals. If the pressure drops below a certain limit, the oscillations are undamped. In this case the local heating can be switched off without the oscillations disappearing. If the pressure is further decreased, the amplitude rises quickly and state B is reached. It was possible in this way to induce low amplitude temperature fluctuations that behave very much like the spontaneous, non-linear temperature fluctuations in state B. This result is important for the theoretical investigation of the instability since it justifies a linear approximation which will be used in a following theoretical treatment.

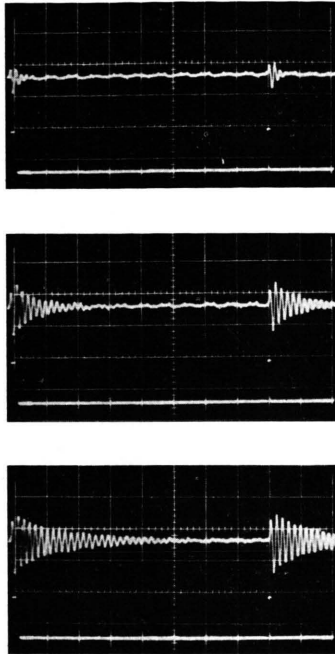


Fig. 17. Damped oscillations of the floating potential of a Langmuir probe (upper trace, horiz. 5 ms/cm) caused by a local microwave heating pulse (lower trace).

10. Measurement of the Radial Electric Field in the Q-PIG Plasma

Because of the electrode geometry of a PIG discharge one can expect an electric field directed towards the axis. Together with the axial magnetic field this field causes a drift in the azimuthal direction that is of great importance in interpreting the experimental results. Some effort was therefore expended in measuring this quantity. Direct measurement of the azimuthal velocity from the Doppler shift of spectral lines (see ¹⁰) failed because the resolution of the spectroscope turned out to be too low. Determination of the field strength from the potential distribution proved to be very erroneous; at best the potential measurements allow the direction of the electric field to be determined. The poor reproducibility of these measurements is apparently due to surface effects on the probes that result in slow

changes of the floating potential. A rotating double probe was therefore used. Its basic design is shown in Fig. 18. The probe could be shifted through the plasma so that any radius in the plasma could be reached. By uniformly rotating the probe about its axis with a frequency of 2 Hz it was possible to eliminate the disturbing influence of the surface effects almost completely.

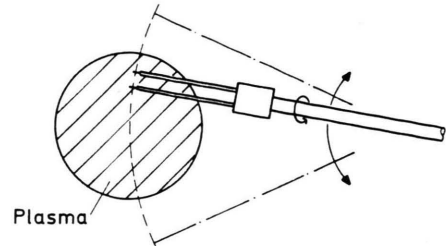


Fig. 18. Sketch of the rotating double probe.

The amplitude of the a. c. voltage picked up from two sliding contacts remained constant for long periods. The maximum field strength measured at, for example, $r \approx 20$ mm (where the temperature maximum usually occurred) was 0.14 V/cm. At $B = 400$ gauss this corresponds to a rotational frequency of 2.8 kHz.

If the field strength is to be determined from the difference between the floating potentials of two probes, one has to assume that the temperature is constant in space and time. This measurement was therefore only possible in the stable state. Comparison, however, between the behaviour of an externally introduced temperature perturbation with the spontaneous temperature fluctuation occurring in state B shows that the two states A and B are not basically different from one another. In particular, the mechanism that causes the rotation of the temperature distribution is most likely the same in both cases, as can be deduced from theoretical considerations. It is therefore assumed that the actual value of the electric field strength in state B does not deviate essentially from that in state A.

11. Qualitative Interpretation of the Experimental Results

The experiments have shown that the states A and B of the Q-PIG plasma differ mainly with respect to the electron temperature distribution perpendicular to the magnetic field. It was also found that the plasma rotates in the same direction and with approximately the same frequency as the region of elevated temperature in state A or the anomalous temperature distribution in state B. Essentially two questions have thus to be answered, namely what causes the anomalous temperature distribution in state B and why does it move in the direction of the $\mathbf{E} \times \mathbf{B}$ drift? In the present paper, which is concerned mainly with the experimental material, only

a few basic aspects are dealt with; a more detailed discussion is reserved for the theoretical paper being in preparation.

One important experimental result was the extremely low electron temperature. Even in the maximum of the temperature distribution (see Fig. 9) the energy of the electrons is still far from sufficient for ionizing neutral helium atoms. For this reason alone there must therefore be a second electron group of much higher energy. It can be shown that these fast electrons are capable not only of ensuring the necessary formation of new charge carriers, but also of heating the slow electrons¹⁰. Furthermore, it was estimated that this heating mechanism exceeds other possible mechanism such as ohmic heating by more than an order of magnitude.

Since the thermal energy of the "cold" electrons is not sufficient either for exciting neutral helium atoms, practically only elastic collision of electrons with ions and neutral particles take place. The energy thereby transferred to the heavy particles per cm^3 and sec thus represents the only energy loss of the electrons. The temperature of the cold electrons is therefore essentially governed by the equilibrium between the heating by the fast electron group and the cooling by elastic collisions with the heavy particles. The energy balance in this case can be formulated as follows:

$$H = 3 \mu n (\nu_{ei} + \nu_{en}) k (T_e - T_i) \quad (2)$$

where H denotes the energy transferred by the fast electrons to the cold electrons per cm^3 and sec, μ the ratio of electron to ion mass, n the plasma density, ν_{ei} and ν_{en} the collision frequencies for elastic collisions between the cold electrons and ions or neutral particles, k Boltzmann's constant, and T_e and T_i the temperatures of the electrons and ions. In addition, we set $T_i \approx T_n$ (temperature of neutral gas) for simplicity. The heating rate H is independent of T_e since the energy of the fast electrons is practically always large compared with the thermal energy of the cold electrons (see also ¹⁰). However, owing to the temperature dependence of the collision frequencies, the right hand side of Eq. (2) depends on the electron temperature in very different ways, depending on which collisions predominate. For low temperatures and high densities ($T_e = 2000^\circ\text{K}$, $n = 10^{12} \text{ cm}^{-3}$) ν_{ei} is of the order of 10^8 sec^{-1} , while for a neutral gas pressure of 30 mTorr ν_{en} is only of the order of 10^7 sec^{-1} . Therefore, in the Q-PIG plasma

collisions between electrons and ions should be highly predominant in state A, i. e. owing to $T_e \gg T_i$ the right hand side of Eq. (2) should essentially be proportional to $T_e^{-1/2}$. In this state, however, the electron temperature is unstable in principle for, because of the temperature independence of H , every increase of T_e leads to less cooling and hence to excessive energy input, i. e. to a further increase in temperature. Let us now consider the development of a local increase in electron temperature. Along the magnetic field lines this perturbation can spread out easily until uniformity is reached. We therefore confine ourselves to the energy balance perpendicular to the magnetic field. If we take into account a transverse heat flux, \mathbf{q}_e , the energy equation has to be extended by the divergence of this heat flux, $\nabla \cdot \mathbf{q}_e$:

$$H = 3 \mu n (\nu_{ei} + \nu_{en}) k (T_e - T_i) - \nabla \cdot \mathbf{q}_e. \quad (3)$$

The term $\nabla \cdot \mathbf{q}_e$ is proportional to $(\nu_{ei} + \nu_{en}) T_e^2$ and inversely proportional to B^2 (for $\nu/\omega_e \ll 1$). The right hand side of Eq. (3) thus depends on two parameters in addition to T_e , viz. the ratio of the collision frequencies ν_{ei}/ν_{en} and the magnetic field. These, however, are the very parameters that were varied for determining the point of transition between the states A and B (see Fig. 13) because at constant temperature and density one has $\nu_{ei}/\nu_{en} \propto \lambda \propto 1/p$. The curve of the experimental points can in fact be explained qualitatively in terms of Eq. (3): For very high neutral gas pressure (λ small) the stabilizing effect of the electron-neutral collisions predominate in the first term of Eq. (3) so that the second term becomes superfluous and the magnetic field has no influence. If, on the other hand, the electron-ion collisions predominate at low neutral gas pressure, a local rise in temperature may possibly be prevented by means of the thermal conduction perpendicular to the magnetic field, and so in a certain pressure range the transition points depend on the magnetic field as well. If, finally, the ratio ν_{ei}/ν_{en} is very large, it depends almost solely on the thermal conduction, i. e. on the magnetic field, whether any temperature perturbation present can be destroyed quickly enough, in accordance with the observation that at low pressure the transition then depends only on the magnetic field and scarcely on the pressure any more. This simple discussion can qualitatively explain the experimental points in Fig. 13.

It remains the question of the motion of the temperature perturbation. At the first glance one might

think of a drift wave like propagation of this perturbation in the electron gas. On the other hand, it may also be localized in the electron gas and simply caught up in the rotation of the plasma. The accuracy with which the radial electric field was measured is not sufficient to determine the state of motion of the temperature perturbation from the experimental observations alone. The experimental results do not disagree, however, with the assumption of a quasi-stationary temperature distribution fixed in the electron gas, an assumption that is largely confirmed by the theory.

12. Comparison of the Q-PIG Discharge with other Discharges

There are several types of discharges that are comparable with the Q-PIG discharge in various respects. The alkali plasmas already mentioned work at low electron temperatures and the drift instabilities are somewhat reminiscent of the instability occurring in the Q-PIG discharge, but that is where the similarity ends. For one thing, the plasma production mechanism is basically different and, for another, the electron and ion temperatures in Q-machines are in general equal. Nevertheless, temperature instabilities may possibly occur in alkali plasmas as well under certain conditions, e. g. when the ion temperature is artificially reduced by adding rare gas (see BLAU et al.¹²).

It is true that the presence of electron groups of various energies is especially characteristic of PIG discharges, but they have also been observed in other discharges. SCHLUETER¹³, for example, found two electron groups in a RF discharge in hydrogen, one group of high energy and low density, another of low energy and high density. The temperature of the latter was about 0.2 eV, similar to that of the cold electrons in the Q-PIG.

Another type of discharge with two different electron groups is the negative glow discharge. A special form of this discharge involving a brush-shaped cathode was developed by PERSSON¹⁴ and investigated in more detail by MOSBURG¹⁵. The plasma of such a discharge is produced by a wide beam of fast

electrons, that are accelerated in the cathode fall region, and is almost free of electric fields. The electrons have a temperature of 0.05 to 0.1 eV and a density of 10^{12} cm⁻³, i. e. collisions between electrons and ions predominate here as well, despite the relatively high neutral gas pressure. The elevation of the electron temperature relative to the neutral gas is ascribed to a heating mechanism in which metastable helium atoms transfer their energy to the electrons by collisions of the second kind. No confining axial magnetic field was used in this discharge.

In none of the discharges described were instabilities observed in which the electron temperature is disturbed. The drift instabilities occurring in alkali plasmas were identified as density fluctuations and therefore differ in character from the instability in the Q-PIG. There is no mention of instabilities in the other papers quoted; but there was evidently no intention of looking for any.

A good number of papers on PIG discharges (see references cited in¹⁰) deal with low frequency instabilities in particular. Most authors describe them as density fluctuations without, however, proving that the electron temperature thereby remains constant. Apparently they all assume that the electron temperature is constant, particularly in the two theoretical papers again quoted here under⁸ and⁹. Only in very few cases is it suggested that the electron temperature may also fluctuate, e. g. by BINGHAM et al.¹⁶. It was recently demonstrated by ZAKRZEWSKI et al.¹⁷ that the electron temperature in a PIG discharge can fluctuate periodically; the paper, however, is concerned mainly with the method of measurement itself and gives no indication of the cause of the observed phenomenon.

13. Summary

In a PIG discharge with modified electrode geometry (Q-PIG) low frequency oscillations (≈ 1 kHz) were observed and identified as fluctuations of the electron temperature. The oscillations only occurred under certain conditions (low gas pressure, relatively high magnetic field), while the plasma was ex-

¹² F. P. BLAU, E. GUILINO, M. HASHMI, and N. D'ANGELO, *Phys. Fluids* **10**, 1116 [1967].

¹³ H. SCHLUETER, *Z. Naturforsch.* **16a**, 972 [1961].

¹⁴ K.-B. PERSSON, *J. Appl. Phys.* **36**, 3086 [1965].

¹⁵ E. R. MOSBURG, *Phys. Rev.* **152**, 166 [1966].

¹⁶ R. L. BINGHAM, F. F. CHEN, and W. L. HARRIES, Rept. Princeton Univ. MATT-63.

¹⁷ Z. ZAKRZEWSKI, C. BEAUDRY, and C. G. CLOUTIER, *Rev. Sci. Instr.* **39**, 1507 [1968].

tremely stable at high pressure and low magnetic field. Near the boundary between the stable and unstable states it was possible to induce similar oscillations of the electron temperature in the stable state as well. A qualitative interpretation of the observed phenomena is obtained from the energy balance of the electron gas, taking into account the thermal conduction perpendicular to the magnetic field. Allowance should be made, moreover, for the fact that the entire plasma rotates in the $\mathbf{E} \times \mathbf{B}$ direction. This model allows the behaviour of the plasma to be explained qualitatively. Finally the Q-PIG discharge is compared with both conventional PIG discharges and various other types of discharges.

This work was undertaken as part of the joint research programme between the Institut für Plasmaphysik und EURATOM.

Acknowledgments

The author is indebted to Prof. R. WIENECKE for his active support and numerous valuable discussions. He is grateful to Dr. G. LANDAUER for various helpful suggestions concerning the experimental approach. His special appreciation goes to Dr. H. M. MAYER and Dr. M. TUTTER for their unfailing readiness to discuss the experimental and theoretical problems involved. Finally, he should like to thank Mrs. G. STÖCKERMANN for her patience and care in evaluating the probe measurements.

Zur Rayleigh-Taylor-Instabilität eines rotierenden Wasserstofflichtbogens im axialen Magnetfeld

H. F. DÖBELE

Institut für Plasmaphysik, Garching bei München

(Z. Naturforsch. 25 a, 273—282 [1970]; eingegangen am 28. November 1969)

The Rayleigh-Taylor instability of a rotating hydrogen arc in an axial magnetic field is investigated with allowance for electrical conduction, heat conduction and viscosity. The r -depending part of the perturbation was assumed to be in the form of a half-period of a standing wave. The corresponding dispersion relation is derived in the WKB-approximation and is solved numerically. In contrast with the case without dissipation, the frequencies and growth rates of the different modes depend on the parameters of the unperturbed plasma column. The calculation shows, in qualitative agreement with the experiment, that with increasing magnetic field the highest growth rate passes successively to the next higher mode.

I. Einführung

In einer früheren Veröffentlichung¹ ist über das Auftreten von Rayleigh-Taylor-Instabilitäten an einem rotierenden Wasserstofflichtbogen mit Hohl-anode in einem axialen Magnetfeld berichtet worden. Der Bogen brannte bei etwa 3–4 Torr über eine Länge von 12 cm zwischen einer Wolframkathode und einer rohrförmigen Anode aus Kupfer. Die Stromstärke betrug für die meisten Messungen 1600 A. Magnetfeldstärken bis 28 kG konnten erreicht werden. Die Rotation wird hervorgerufen durch die $\mathbf{j} \times \mathbf{B}$ -Kraft, die mit der radialen Stromdichtekomponente in der Anode verbunden ist. Die Rotationsgeschwindigkeit wurde aus dem Doppler-Effekt der Linie 3995 Å des in geringer Menge zugefügten Stickstoffs bestimmt. Sie erreicht am Bogenrand den Wert $2,8 \cdot 10^6$ cm/sec. Die Instabilität zeigt sich in Form von periodischen Lichtintensitäts-

schwankungen der vom Bogenrand ausgehenden Strahlung. Die beobachteten Frequenzen liegen je nach Magnetfeldstärke zwischen 0,9 und 1,45 MHz und entsprechen den Moden $m=4$ (bei 16 kG) bis $m=7$ (bei 26 kG). Die Amplituden erreichen maximal 10% des Intensitätsmittelwertes. Die verschiedenen Moden wurden durch „end-on“-Beobachtung der Phasenlage der Signale am Bild des Innenrandes der Anode mit zwei Photomultipliern und nachfolgender Korrelationselektronik identifiziert. Man findet, daß die azimutale Wellenzahl m in der Weise von der Magnetfeldstärke abhängt, daß mit steigender Feldstärke nacheinander höhere Moden auftreten. Durch Beobachtung der Störungen unmittelbar vor beiden Elektroden findet man, daß bei voll ausgebildeter Instabilität keine meßbare Verschraubung besteht; d. h. es liegt eine „Flute“-Instabilität vor mit parallel zu den Magnetfeldlinien verlaufenden Störungen.

Sonderdruckanforderungen an Dr. H. F. DÖBELE, Institut für Plasmaphysik, D-8046 Garching bei München.

¹ H. F. DÖBELE, Z. Naturforsch. 24 a, 1249 [1969].